Ultrasound enhanced synthetic platelet therapy for augmented wound repair

Seema Nandi[1,2], **Kaustav Mohanty**[3], **Kimberly Nellenbach**[1,2], **Mary Erb**[1], **Marie Muller**[1,3], **Ashley C. Brown**[1,2,*]

[1]Joint Department of Biomedical Engineering, North Carolina State University and The University of North Carolina at Chapel Hill, Raleigh, NC

[2]Comparative Medicine Institute, North Carolina State University

[3]Department of Mechanical and Aerospace Engineering, North Carolina State University
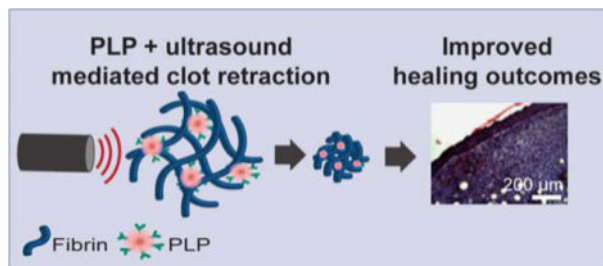
Abstract

Native platelets perform a number of functions within the wound healing process, including interacting with fibrin fibers at the wound site to bring about retraction after clot formation. Clot retraction improves clot stability and enhances the function of the fibrin network as a provisional matrix to support cellular infiltration of the wound site, thus facilitating tissue repair and remodeling after hemostasis. In cases of traumatic injury or disease, platelets can become depleted and this process disrupted. To that end, our lab has developed synthetic platelet-like particles (PLPs) that recapitulate the clot retraction abilities of native platelets through a Brownian-wrench driven mechanism that drives fibrin network densification and clot retraction over time, however, this Brownian-motion driven process occurs on a longer time scale than native active actin/myosin-driven platelet-mediated clot retraction. We hypothesized that a combinatorial therapy comprised of ultrasound stimulation of PLP motion within fibrin clots would facilitate a faster induction of clot retraction on a more platelet-mimetic time scale and at a lower dosage than required for PLPs acting alone. We found that application of ultrasound in combination with a subtherapeutic dosage of PLPs resulted in increased clot density and stiffness, improved fibroblast migration *in vitro* and increased epidermal thickness and angiogenesis *in vivo*, indicating that this combination therapy has potential to facilitate multiphase pro-healing outcomes. Additionally, while these particular studies focus on the role of ultrasound in enhancing specific interactions between fibrin-binding synthetic PLPs embedded within fibrin networks, these studies have wide applicability in understanding the role of ultrasound stimulation in enhancing multi-scale colloidal interactions within fibrillar matrices.

Graphical Abstract

*Correspondence:** Ashley C. Brown, PhD, Joint Department of Biomedical Engineering, University of North Carolina at Chapel Hill/North Carolina State University, 1001 William Moore Dr., Raleigh, NC, 27607, aecarso2@ncsu.edu.

Supporting Information: Supporting information is available and is comprised of figures demonstrating the following: 1) Representative force maps of fibrin clots in the presence or absence of ultrasound; 2) Comparison of PLP + US and hard (10% BIS) fibrin-targeting particle effects on clot density; 3) Comparison of PLP + US and native platelet effects on clot density; 4) Comparison of PLP + US and native platelet effects on clot stiffness; and 5) Representative images of "wounded" area in fibroblast migration assay.

PLP + ultrasound mediated clot retraction

Improved healing outcomes

200 μm

Fibrin ∴ PLP

Keywords

Biomimetic; fibrin; wound healing; clot retraction; artificial platelet

Introduction

Native wound healing is a complex process involving the orchestration of multiple biological cues and interactions. Upon vessel injury, circulating platelets become activated and marginate to injured vasculature[1], interacting with fibrin forming at the injury site to form a platelet-fibrin "plug." Platelets then utilize actin-myosin machinery to pull on the bound fibrin fibers, expelling serum from and stabilizing the clot in a process known as clot retraction[2]. Fibrin forming at the wound site serves as a provisional matrix scaffold for supporting cellular infiltration requisite for tissue repair; clot retraction aids in this process by bringing about increased clot density and stiffness, stabilizing the provisional fibrin network and supporting its ability to facilitate cellular infiltration and the synthesis of new extracellular matrix[3–4]. Previous studies by our lab indicate that this increase in clot stiffness plays a role in enhancing cell migration into the clot matrix and in enhancing subsequent healing markers in the injured tissues[5].

In cases of traumatic injury or disease, platelets can become depleted or dysfunctional, impairing clot retraction and the ensuing wound healing processes[6–7]. To this end, our group has developed highly deformable synthetic platelet-like particles (PLPs) that are capable of recapitulating the fibrin binding and clot retraction abilities of native platelets[8]. While native platelet-mediated clot retraction occurs via active actin/myosin driven processes, PLP-mediated clot retraction occurs due to a unique Brownian wrench driven mechanism that is dependent on the highly deformable nature of the ultra-low crosslinked (ULC) microgels comprising the particles and the high fibrin binding affinity imparted by the fibrin-binding antibody coupled to the particles. PLPs are comprised of highly deformable ULC poly (N-isopropylacrilamide-co-acrylic acid) (pNIPAM) microgels covalently coupled to a fibrin-binding antibody. The microgel "body" of the PLPs mimic the size of native platelets (~1 μm in solution) and, due to the highly deformable nature of the ULC microgel, is capable of undergoing extreme morphological changes which we have previously shown to mimic the extensive shape change associated with native platelet activation following injury[5]. This highly deformable nature of the ULC microgels allows for PLPs (i.e. ULC microgels coupled to a fibrin-binding antibody) to spread extensively within fibrin networks once clot formation occurs, thereby allowing for one particle to interact with multiple fibrin fibers. These interactions are critical to PLP-mediated clot retraction. PLPs are stretched as they

bind fibers within a fibrin network, then collapse inward to return from a stretched conformation to a more energetically favorable spherical conformation, pulling the fibers with them and creating microcollapses in the clot network that build to create an overall clot retraction event (Figure 1). This mechanism of PLP-fibrin network interaction, shape change, and subsequent fibrin network microcollapse leading to bulk clot retraction has been observed and characterized previously[8]. Studies characterizing this mechanism have indicated that local alternations in fibrillar microstructure are highly dependent on particle adhesiveness and the compliance of the particles themselves. These studies demonstrated that the soft, deformable ULC microgels coupled to a fibrin-targeting motif to form PLPs are able to sufficiently adhere to the network to a degree necessary to overcome the energy threshold needed to induce fibrin network collapse[8]. Additional previous studies by our group have shown that PLP-mediated clot retraction results in enhanced clot stiffness and structure, as well as in increased cell migration in an *in vitro* model of wound healing and enhanced markers of wound healing in a murine full-thickness dermal injury model[5].

Despite these improvements in clot properties and wound healing responses, application of PLPs to clot matrices both *in vitro* and *in vivo* are limited in the time scale of their responses. Importantly, native platelet-induced clot retraction is an active actin/myosin driven process which occurs within a matter of hours[2, 9]; in contrast, PLP-induced clot retraction (when studied within a purified fibrinogen + thrombin clot system) occurs over a longer time scale, with full clot retraction taking up to 24 hours to observe[5]. The rate of PLP-mediated clot retraction can be controlled to some degree via passive methods of increasing fibrin/PLP interactions, for example by increasing the PLP concentration or increasing the availability of fibrin-targeting motifs on the PLPs. However, such approaches are likewise limited by the Brownian motion of the PLPs. To address these limitations, we investigated the application of an active stimulation mechanism to PLP-laden clot matrices to determine if the previously observed clot retraction and improved wound healing responses could be achieved using a lower dosage of PLPs than previously required (Figure 1). Studies conducted on the application of ultrasound to ULC microgels have indicated that ultrasound treatment increases deformation and motion of ULC microgels within a tissue-mimicking phantom[10]. Therefore, in these studies, we applied active stimulation to PLPs within a clot matrix using ultrasound and hypothesized that, due to the previously observed increase in ultrasound-induced deformation of ULC particles within a tissue-like phantom, the combination of ultrasound treatment with PLPs would result in improved clot retraction and wound healing responses both *in vitro* and *in vivo* at a lower requisite dosage than would occur for PLPs applied alone. Overall, our results show that application of ultrasound in combination with a subtherapeutic dosage of PLPs resulted in increased clot density and stiffness, indicative of clot retraction, as well as in improved fibroblast migration *in vitro* and increased epidermal thickness and angiogenesis *in vivo*. Taken together, these results indicate that this combination therapy has potential to facilitate multiphase prohealing outcomes using lower doses of PLPs than had been previously achieved.

Results and Discussion

ULCs mimic the deformability and size of native platelets

ULC microgels were synthesized via a precipitation polymerization reaction of NIPAM and acrylic acid. Previous studies utilizing ULC microgels synthesized via this method show that the resultant micro-scale hydrogel particles exhibit key properties similar to those of native active platelets; in particular, these ULC microgels have been shown to exhibit high degrees of deformability upon glass surfaces as well as similar sizes to those of active platelets[5, 8]. We first confirmed that ULC microgels synthesized for these studies exhibited similar size and deformability upon glass surfaces using dynamic light scattering (DLS) and atomic force microscopy (AFM) imaging. DLS analysis of ULC microgels as performed using a Malvern Zetasizer Nano S revealed that ULC microgels suspended in 10 mM HEPES buffer (pH 7.4) had a hydrodynamic radius of 1.22 ± 0.11 μm, and AFM dry imaging of ULC microgels deposited on a glass coverslip revealed that they flattened to a height of 26.5 ± 21.7 nm (Figure 2). These results indicate that the ULC microgels synthesized here remain consistent with previously synthesized ULC microgel morphology and mimic the deformability and size of native platelets (Figure 2).

Application of ultrasound and PLPs in combination increases clot density and stiffness

Upon conjugation of ULC microgels to anti-fibrin fragment E antibodies to form PLPs, PLPs are able to bind fibrin fibers within the clot and take on spread conformations within fibrin networks. As the microgels return to spherical conformations, this causes the bound fibers to be pulled inward, leading to microcollapses in the clot network structure and ultimately overall clot retraction. However, while previous applications of PLPs did indeed recapitulate the clot retraction and stiffening responses that occur in native platelet-mediated wound healing, these PLP-mediated responses happened over a much longer time scale than would occur with native platelet-mediated responses. We sought to increase the rate of this phenomenon via the application of an external active stimulation method (ultrasound) to PLPs within a fibrin network. We hypothesized that when ultrasound is applied to PLP-incorporated clots, PLP motion will be enhanced within the network, resulting in a faster rate of PLP-fibrin binding and causing clot retraction to occur on a faster time scale than observed when applying PLPs alone (Figure 1). In these studies, we utilize a 0.025 mg/ml concentration of PLPs, which was the concentration of particles found to achieve maximum motion within a tissue-like phantom when subjected to an optimal 1 MHz ultrasound frequency[10]. Since this concentration is an order of magnitude lower than the 0.5 mg/ml concentration of PLPs that was found optimal for inducing clot retraction and improved cell migration and wound healing in previous studies[5], we expected that the application of this lower concentration of PLPs in the absence of ultrasound stimulation would have minimal effect on clot contraction and on subsequent healing responses. Previous studies involving the application of ultrasound to the ULC microgels used in this study to form PLPs have demonstrated that ultrasound induced rapid particle deformations, with frequencies corresponding to the ultrasound excitation frequencies (in the MHz range)[10]. As a result of these rapid particle deformations, we postulate that the rate of PLP-fibrin interactions is increased relative to the Brownian motion-dependent rate of PLP-fibrin interactions that occur in the absence of ultrasound stimulation. When this rate of interaction increases, the

PLPs become spread within fibers and take on an energetically unfavorable 'spread' conformation more quickly than they would when applied within a fibrin matrix alone. Due to the energetically unfavorable nature of this conformation, the PLPs then collapse back into a more favorable spherical conformation, "pulling" the bound fibrin fibers as they collapse. This mechanism of PLP shape change and subsequent clot network contraction has been studied and characterized previously[8].

We first investigated the ability of a combinatorial ultrasound and PLP application to enhance fibrin clot density in a manner reminiscent of native platelets through confocal microscopy analysis of fibrin clots formed in the presence or absence of PLPs with or without ultrasound stimulation following clot polymerization. Clots were allowed to polymerize for 1 hour, then ultrasound stimulation was added for 30 minutes. Clots were analyzed via confocal microscopy, 2 hours after initial clot formation (30 minutes after application of ultrasound). Utilizing a much lower concentration (~10 fold lower) of PLPs than the optimal concentration from studies utilizing PLPs alone[5], we found that clot density was significantly enhanced in the presence of both PLPs + ultrasound (US) relative to controls (fibrin-only clots +/− US, non-fibrin targeting ULC microgel clots +/− US, PLP clots - US) when measured two hours after initial clot formation (Figure 3). This can be compared to previous findings, which showed enhanced network density in the presence of PLPs in clots imaged 24 hours after initial clot formation[5], demonstrating that the application of ultrasound to PLP-laden clots results in PLP-mediated clot retraction at much lower doses and faster time scales than previous observed; clot density in our low-concentration PLP + US group was determined to be 1.16 ± 0.7 at 2 hours after initial clot formation, whereas clot density in our previously studied higher concentration PLP group alone was determined to be 1.47 ± 0.5 24 hours after initial clot formation[5]. In order to evaluate the theory that PLP deformability under ultrasound stimulation is a key factor in this observed increase in clot density, we compared PLP-laden clot densities with the densities of clots incorporated with a stiff (10% BIS) microgel coupled to the fibrin-targeting antibody used to create PLPs. Results from application of US to clots containing stiffer 10% BIS-Frag E particles reveal significantly lower clot densities than those observed in the presence of more deformable PLPs + US (Figure S2). Furthermore, we observed that application of PLPs + US to fibrin clots resulted in clot densities similar to that observed in clots containing native platelets + US (Figure S3).

Results from the fibrin + US group indicate a slightly diminished effect on clot density when ultrasound is applied to fibrin-only clots in the absence of PLPs; this is consistent with previously published data that shows that ultrasound can be applied to clots in order to induce fibrinolysis[11–13]. Due to the fact that the PLP + US clots still have improved network structure over standard fibrin clots, we posit that the effect of US on the PLPs within these matrices is influencing the clot matrices to a greater degree than that of the ultrasound on fibrin alone. Interestingly, clots containing ULC microgels that were exposed to ultrasound displayed improved clot structure over ULC microgel-laden and PLP-laden clots in the absence of US. There are a few possible reasons that these clots displayed improved clot density over PLP – US clots. This could largely be due to the fact that the PLP concentration used in these studies is severely sub-optimal relative to the previously discovered 0.5 mg/ml concentration of PLPs needed to induce improvements in clot structure[5]; therefore, it is

expected that no significant improvements in clot density would be observed using this lower concentration of PLPs alone. Additionally, our previous studies by Joshi *et al.* have demonstrated that application of US results in movement of ULC microgels within a tissue-like phantom[10], so the results observed in the ULC microgel + US group could be a simple physical effect in which moving particles within the clot matrix results in a small degree of rearrangement of the network. Nonspecific charge interactions between the acrylic acid groups on the ULC microgels and the fibrin fibers within the clot network could also be somewhat contributing to the observed improvement in network density over the PLP – US group. However, the observed increase in clot density over standard fibrin clots are stronger in US-treated groups that have the fibrin binding element present (PLP + US), highlighting the contribution of the fibrin-binding feature of PLPs on fibrin density beyond any non-specific contributions of non-binding particles.

We additionally investigated the time scale and effect of the combinatorial PLP + ultrasound treatment on clot stiffness using AFM force mapping. Force maps obtained two hours after initial clot formation demonstrated that clots subjected to both PLPs + ultrasound conditions exhibited significantly greater Young's moduli than control clots ($p < 0.0001$ vs. Fibrin (−) US, ULC microgel (−) US, ULC microgel (+) US, and PLP (−) US clots; $p = 0.0023$ vs. Fibrin (+) US clots); Figure S1, Figure 4). The moduli determined two hours after initial formation for clots exposed to both PLPs and ultrasound (2.82 ± 0.49 kPa) was found to be similar to the previously published moduli determined 24 hours after initial formation for clots exposed to a higher dosage of PLPs acting alone (2.47 ± 0.51 kPa)[5], indicating that application of PLPs in combination with ultrasound can bring about clot retraction and stiffening responses at a similar level to those observed previously on both an order of magnitude lower time scale and concentration than previously required using PLPs alone. As expected, application of a subtherapeutic dosage of PLPs without the combined ultrasound stimulation produced network density and stiffness values on par with those observed in control fibrin clots, signifying that the combination of both PLPs and ultrasound stimulation are necessary to achieve this quickened clot retraction response. Additionally, when compared to the stiffness of clots formed from native platelets +/− US, clots formed from PLPs + US did not exhibit significant differences in Young's moduli relative to clots formed using platelets + US, nor did clots formed from PLPs in the absence of US significantly differ from clots formed from platelets in the absence of US (Figure S4).

Ultrasound and PLP treatments increase cell migration in an in vitro model of early cell migration

A large body of work published over the last decade indicates that increased matrix stiffness drives cellular migration[14–15], and previously published studies from our group have demonstrated increased fibroblast migration within relatively stiffer PLP-laden fibrin clot matrices in comparison with migration within less stiff control fibrin clot matrices[5]. Given these results and the lowered time scale and requisite concentration required to increase clot stiffness in the presence of PLPs + ultrasound treatment, we hypothesized that fibroblast migration within an *in vitro* model of wound healing would be enhanced in the presence of fibrin clots exposed to combined PLPs + ultrasound exposure relative to migration in the presence of control clots. We evaluated fibroblast migration in the presence of PLP +

ultrasound treated clots by seeding fibroblasts within a collagen/fibrinogen matrix, inducing a defect into the matrix to simulate an injury, and filling the defect with a fibrin clot matrix. PLPs or ULC microgels were added into the clot matrix per experimental condition. Clots were allowed to polymerize for 1 hour and + ultrasound groups were subsequently exposed to 30 minutes of ultrasound stimulation. Fibroblast migration into the wound area was characterized immediately after induction of the defect and 2 hours after induction of the defect via microscopic evaluation. Fibroblast migration into the defect area after 2 hours was found to be significantly increased in the PLP + ultrasound group relative to migration in all control conditions (p < 0.0001 relative to all groups) (Figure 5, Figure S5), indicating that the PLPs + ultrasound treatment brings about enhanced early fibroblast migration within this *in vitro* model of wound healing, at much earlier time scales than previously observed with PLPs in the absence of active ultrasound stimulation[5]. Cell counts in the PLP + ultrasound group were found to be 10 ± 3 two hours after clot formation, while mean cell counts in the control groups were as follows: PLP – ultrasound: 4 ± 1; ULC microgel + ultrasound: 4 ± 1; ULC microgel – ultrasound: 3 ± 2; fibrin + ultrasound: 3 ± 1; and fibrin - ultrasound: 3 ± 3 fibroblasts in the defect area two hours after initial clot formation and application of ultrasound to relevant groups. As observed in the confocal microscopy and atomic force microscopy results, the suboptimal dosage of PLPs alone did not have significant effects on fibroblast migration within this model, as expected based on our previous studies.

The significant increase in fibroblast migration in samples treated with PLPs + ultrasound indicates that this combination treatment allows early cell migration. Early migration of fibroblasts into a wound site is critical for the development of a functional extracellular matrix to support later stages of wound healing[16], so the enhanced early fibroblast migration response seen in this model after combinatorial application of PLPs and ultrasound indicates that this combination treatment could additionally improve subsequent wound healing responses beyond initial fibroblast migration into the wound area. It is likely that the mechanical properties of the clots within the defect areas are not the only factor causing this increase in fibroblast migration in the PLP + US group; the model developed for this study is highly simplified and does not account for cytokine gradients, fibroblast phenotypic changes or secretome responses that would occur during the cellular migration and proliferation phase, or other biological and biochemical factors that would typically influence cellular behavior within an *in vivo* wound site. In this simplified model, we postulate that the differences in modulus between the collagen/fibrinogen matrix (198 ± 190 Pa) and the clots treated with PLP + US (2820 ± 490 Pa) promote increased fibroblast migration within the PLP + US group in part due to a durotactic effect in which a stiffness gradient is appearing between the collagen/fibrinogen matrix and the provisional fibrin clot matrix within the defect.

Ultrasound + PLP combination therapy enhances wound healing events in a murine dermal injury model

Reports suggest that native platelets play a role in augmenting wound healing by inducing clot retraction and facilitating blood reperfusion to injured tissues[3, 17]; additionally, the previously observed ability of PLPs to induce clot retraction likewise enhances fibroblast migration within provisional fibrin matrices, which would allow for fibroblasts to proliferate

within the wound environment and synthesize new extracellular matrix to repair the injured tissue. These events could lead to the enhanced angiogenic responses and increased epidermal thickness of previously observed in wounds treated with PLPs[5]. In this study, we hypothesized that the combined application of both ultrasound and a low (sub-therapeutic) dosage of PLPs could likewise enhance wound healing in an *in vivo* murine full thickness dermal injury model. Due to the clot retraction and fibroblast migration responses obtained using PLPs and ultrasound in combination, we proposed that this combination therapy could likewise bring about improved wound healing responses *in vivo* using a much lower dosage of PLPs than was previously required to obtain this effect. As this model was utilized in healthy mice with normal coagulation systems, we expect that there would also be some degree of contribution to wound healing from native platelets and fibrinogen; indeed, previously published data utilizing this full thickness dermal injury model indicate that PLPs applied to full thickness dermal wounds incorporate with native fibrin forming at the wound sites[5, 18], indicating that normal coagulation process are taking place as well. The studies presented herein were designed to understand the effect of the PLP + US interaction in an *in vivo* system; future works in this area may focus on application of this system within animals exhibiting dysfunctional coagulation or healing in order to study the effect of this treatment in more complex cases.

Saline or fibrin clots ± PLPs or non-binding ULC microgel controls were applied to wounds. Clots were applied in suspension to the wounds to allow the clots to polymerize at the wound sites themselves, rather than polymerizing and retracting prior to application. Wounds were then treated with ultrasound for 30 minutes and monitored for 9 days prior to being collected for histological analysis (Figure 6a–b). Control groups included application of saline or fibrin clots ± PLPs or non-binding ULC microgel controls without ultrasound application. Wound closure percentages revealed that PLP + ultrasound treatment groups showed relatively greater closure percentages, though not statistically significant, at early time points relative to all other treatments (Figure 6c). Although no significant differences were observed in overall wound closure 9 days after injury, histological analysis reveals significant differences in wound healing markers within these tissues. It is possible that statistical differences in wound closure were not observed in groups in this study due to either small initial wound sizes or small sample sizes. Due to the relatively small size of the animals used in this study, creation of larger wounds was not logistically feasible. This is a limitation of the study, and future work in this area may involve the utilization of a larger rodent model, such as a rat model, in order to allow for the creation and observation of wound closure rates using larger initial wound sizes and to determine if larger initial wound sizes would allow for macroscopic visualization of wound healing differences.

Histological analysis of wound tissues collected 9 days post-injury revealed significantly enhanced epidermal layer thickness (as determined from MSB images) and angiogenesis (as marked by CD31 positively-labeled tissue) for wounds treated with a combination of PLPs and US relative to all controls, indicating improved markers of wound healing in this treatment group (Figure 6d–f). For the PLP + ultrasound group, average epidermal thickness was found to be 62.2 ± 8 μm. In contrast, PLP – ultrasound groups showed average epidermal thicknesses of 17.3 ± 17 μm (p = 0.0023 relative to PLP + ultrasound), ULC microgel groups treated with and without ultrasound had average epidermal thicknesses of

20.5 ± 12 μm (p = 0.0052 relative to PLP + ultrasound) and 24.1 ± 18 μm (p = 0.0127 relative to PLP + ultrasound), respectively, fibrin groups treated with and without ultrasound had average epidermal thicknesses of 15.0 ± 11 μm (p = 0.0013 relative to PLP + ultrasound) and 27.8 ± 26 μm (p = 0.0305 relative to PLP + ultrasound), respectively, and saline-only controls had average epidermal thicknesses of 8.52 ± 13 μm (p = 0.0002 relative to PLP + ultrasound). IHC labeling for angiogenesis indicator CD31 revealed that the PLP + ultrasound group averaged 6050 ± 6800 $μm^2$ of CD31+ area. Conversely, PLP – ultrasound groups averaged 11.3 ± 17 $μm^2$ of CD31+ area (p = 0.0006 relative to PLP + ultrasound), ULC microgel groups with and without ultrasound averaged 147 ± 86 $μm^2$ (p = 0.0008 relative to PLP + ultrasound) and 66.3 ± 71 $μm^2$ (p = 0.0004 relative to PLP + ultrasound), fibrin groups with and without ultrasound averaged 1120 ± 700 $μm^2$ (p = 0.0058 relative to PLP + ultrasound) and 29.2 ± 28 $μm^2$ (p = 0.001 relative to PLP + ultrasound), and saline groups averaged 107 ± 97 $μm^2$ (p = 0.0005 relative to PLP + ultrasound). The significant increase in these markers of wound healing in tissues exposed to this combination therapy, in conjunction with the relatively greater rate of wound closure relative to most other groups, indicate a faster and more robust healing response in response to the combination therapy of both PLPs and ultrasound together.

We next evaluated macrophage infiltration and phenotype within the wound tissue. Macrophage labeling of wound tissues using antibodies to pan-macrophage marker CD68, M1-like macrophage marker CD86, and M2-like macrophage marker mMMR/CD206 revealed potential differences in macrophage polarization across groups, although further studies would be required to draw conclusive results as to the effects of these treatments on macrophage response within the wound area 9 days after injury. Immunolabeling for macrophage polarization revealed different trends among groups treated with saline, fibrin, ULC microgels, and PLPs, as well as among groups that received ultrasound and groups that did not; however, no significant difference exists among groups (Figure 7). In general, the macrophage response in the PLP group appears somewhat muted in tissues collected 9 days after application of ultrasound, however, no statistically significant differences were found. While it seems that differences might exist as a result of the varied treatments applied to these wounds, further experimentation would be necessary in order to definitively evaluate the macrophage responses in wound tissue across various particle type and ultrasound treatment groups. However, as no significant differences were observed between groups, we cannot yet draw conclusions about the effect of PLP treatment on the macrophage response within these types of wounds, and further characterization of the M1/M2 phenotype would be necessary prior to doing so.

Conclusions

The overall purpose of this study was to determine if combinatorial application of PLPs and ultrasound could enhance pro-healing effects relative to fibrin-only controls and to low treatment doses of PLPs alone in *in vitro* and *in vivo* models of wound healing. This was assessed via characterization of clot structural and mechanical properties, *in vitro* cell migration assays, and an *in vivo* full thickness dermal injury model of wound closure. In these studies, we demonstrated that incorporation of PLPs within fibrin clot matrices both *in vitro* and *in vivo* result in enhanced clot retraction, clot stiffness, fibroblast migration *in*

vitro, and wound healing markers *in vivo* when applied in conjunction with ultrasound stimulation. The clot retraction responses observed using this combinatorial technique occur on an order of magnitude shorter time scale than the time scale required when applying PLPs alone (2 hours vs. 24+ hours), allowing for better recapitulation of the time scale of platelet-induced clot contraction than had previously been achieved. The order of magnitude lower dosage of PLPs required to achieve these results (0.025 mg/ml vs. 0.5 mg/ml previously) is also highly advantageous, as it means a much lower supply of PLPs would be needed in order to achieve improved *in vivo* healing outcomes, which could in turn lower the costs of treatment when applied to larger animal models and humans. Although the mechanism of ultrasound-PLP interaction is unlikely to be the sole occurrence responsible for the enhanced healing outcomes observed in these studies, the data presented herein, in conjunction with our previous data illustrating the effects of PLPs on fibrin networks and the effects of ultrasound excitation on microgels, indicates that the effect of ultrasound on the PLPs contributes to increased deformation of PLPs within the fibrin network, leading to enhanced clot retraction. Due to the results of previous studies that have shown that PLPs are capable of inducing clot retraction and matrix stiffening[5, 8], and due to results that have shown that cellular behaviors and overall healing responses seem to correlate with stiffer, retracted fibrin matrices[5, 18], we expect that this PLP-US induced stiffening of the fibrin matrix partially drives enhanced healing responses via durotactic mechanisms. However, because the mechanisms of interaction between ultrasound and PLPs responsible for enhanced healing outcomes are likely much more complex than this single mechanism, more detailed investigations into interactions between PLPs, ultrasound, and wound healing responses will be the subject of future studies. The ability of a low dosage of PLPs to induce clot retraction on a more platelet-mimetic time scale when applied in combination with ultrasound and to support multiple phases of wound healing, from clot contraction through fibroblast migration and tissue repair, indicates that this combination therapy has the ability to serve as a biomimetic platform for facilitating wound healing responses across multiple time and length scales. Additionally, these studies demonstrate that ultrasound stimulation to deformable microgels has the potential to enhance their functionality. While these particular studies focus on the role of ultrasound in enhancing specific interactions between fibrin-binding synthetic PLPs embedded within fibrin networks, these studies have wide applicability in understanding the role of ultrasound stimulation in enhancing multi-scale colloidal interactions within fibrillar matrices.

Methods

PLP formation and characterization

Ultralow crosslinked (ULC) poly(*N*-isopropylacrylamide-*co*-acrylic acid) (pNIPAm) microgels were synthesized in a precipitation polymerization reaction under nitrogen, as described previously[5]. NIPAm and acrylic acid were dissolved at a 90:10 weight ratio in ultrapure water at a total monomer concentration of 140 mM. Acrylic acid was incorporated into the monomer solution to provide functional groups on the microgels; these functional groups allowed for coupling of fibrin-binding antibodies following microgel formation and purification. The synthesis reaction was initiated using 1 mM ammonium persulfate and allowed to run for 6 hours at 70 °C under constant stirring at 450 rpm. Microgels were

filtered through glass wool and purified via dialysis against ultrapure water. Microgel size and spreading behavior was characterized by atomic force microscopy dry imaging of microgels deposited on a glass surface using an Asylum MFP 3D Bio atomic force microscope, as published previously[5]. Following microgel purification, lyophilization, and resuspension in ultrapure water, microgels were covalently coupled to a sheep anti-human fibrin fragment E polyclonal IgG antibody (Affinity Biologicals, Ancaster, ON, CAN) using EDC/NHS chemistry. EDC (50 mg/ml) and NHS (5 mg/ml) were diluted 10X into ultrapure water and incubated with 3.625×10^{-2} mg ULCs for 30 minutes. 1 mg of antibody was then added to the ULC suspension, and the reaction was carried out for 4 hours prior to purification via dialysis against ultrapure water. Purified PLPs were lyophilized and resuspended in ultrapure water (for *in vitro* experiments) or 0.9% sterile filtered saline (for *in vivo* experiments) at the desired concentrations for each experiment.

Additional 10% crosslinked microgels were synthesized as described above, but with the addition of N,N'-methylenebisacrylamide (BIS) to the NIPAM and AAc monomer solution at a final weight ratio of 80:10:10 NIPAM:BIS:AAc. 10% BIS microgels were filtered, purified via dialysis, and coupled to an anti-fibrin fragment E antibody as described above.

Fibrin clot formation and ultrasound application

We previously described experiments to determine optimal ultrasound parameters for maximizing particle deformation within clots by embedding a range of particle concentrations (0.005 mg/mL to 0.040 mg/mL) into tissue-mimicking agar-gelatin phantoms and observing secondary particle motion within the phantom over a range of applied ultrasound frequencies (0.5 to 4.0 MHz)[10]. Continuous sine-wave signals with a peak-to-peak pressure of 2 MPa were generated using a Keysight arbitrary waveform function generator (Keysight Technologies, Santa Rosa, CA, USA) and delivered via single element plane immersion transducers at a range of central frequencies (Olympus Scientific Solutions, Waltham, MA, USA). Signals were delivered via burst cycles of 10 μs on /240 μs off. Maximal particle motion was obtained at a frequency of 1 MHz and 0.025 mg/mL particles, and these parameters were applied for all experiments described herein.

Control fibrin clots created for the present studies were formed using 2 mg/mL human fibrinogen (FIB 3, Enzyme Research Laboratories, South Bend, IN, USA) and 0.1 U/mL human α-thrombin (Enzyme Research Laboratories, South Bend, IN, USA) in HEPES buffer (10 mM HEPES, 150 mM NaCl, 2.5 mM $CaCl_2$, sterile filtered, pH 7.4). For confocal microscopy, Alexa-fluor 488 labeled fibrinogen comprised 10% of the total fibrinogen content for visualization of clot structure. Clots containing non-binding ULC microgels were created to serve as a negative control for the fibrin-binding abilities of PLPs within clots and contained 0.025 mg/mL unconjugated ULCs. Likewise, fibrin-binding PLP clots contained an 0.025 mg/mL PLPs. Control clots formed for confocal microscopy were also created as described, with the addition of 0.025 mg/ml 10% BIS-Frag E particles (10% crosslinked microgels coupled to fibrin fragment E-targeting antibodies). Additional clots for confocal microscopy and AFM were formed using platelets reconstituted in Tyrode's buffer to serve as a positive control. Platelets were obtained by collecting whole blood via venipuncture, centrifugation at $800 \times$ g for 8 minutes to isolate PRP. Platelets were counted and

resuspended in Tyrode's buffer, then embedded into fibrin clots at a final concentration of 150,000 platelets/μL. Blood collection was performed under a protocol approved by the Institutional Review Boards of both the Durham Veterans Affairs and Duke University Medical Centers. All clot measurements for each experiment described herein were taken 2 hours after initial clot formation to allow for 1 hour of initial clot polymerization, 30 minutes of ultrasound application, and any sample incubation time needed per instrument.

Evaluation of PLP + ultrasound combinatorial treatment on clot structure

Control fibrin clots, non-binding ULC containing clots, and PLP containing clots were created as described above and polymerized onto glass microscope slides. Additional clots containing either platelets or 10% BIS-Frag E particles were also created. For fibrin + ultrasound (US), ULC + US, PLP + US, platelet + US, and 10% BIS-FragE + US clot groups, ultrasound was applied to clots for 30 minutes following a 1 hour polymerization period, as described above. Clots were covered with glass coverslips and imaged using a Zeiss Laser Scanning Microscope (LSM 710, Zeiss Inc., Jena, GER) at a magnification of 63X to determine differences in clot structure in the presence of US for each treatment condition[19]. 5.06 μm z-stacks were taken in three random locations per clot, and five clots were imaged per condition. Z-stacks were processed into 3D projections and binarized using ImageJ image analysis software with a threshold of 150–255 (National Institutes of Health, Bethesda, MD, USA). Following binarization, fibrin fibers appeared black and negative space appeared white[5, 20]. Fiber density was determined by dividing the total area of black pixels by the total area of white pixels; fiber density ± standard deviation is reported for each group.

Evaluation of clot stiffness in the presence of PLPs + ultrasound

Clot stiffness was determined in the presence of PLPs ± US, ULCs ± US, platelets ± US, or control fibrin ± US via atomic force microscopy (AFM) (Asylum MFP-3D Bio, Asylum Research, Santa Barbara, CA, USA) operated in contact force mode using silicon nitride cantilevers with a particle diameter of 6.01 μm (Nanoandmore, Watsonville, CA, USA). AFM software Igor Pro 15 was used to determine the spring constant of each cantilever. Three random 10 μm × 10 μm force maps comprising 256 force curves each were taken per clot, and a minimum of three clots were measured per group. The Hertz model, which calculates the Young's modulus of a material based on the Poisson's ratio value of the sample and on the cantilever tip geometry and material, was applied over the linear region of a representative force curve to fit each force map in order to obtain the Young's modulus for each force curve within the force map. For the clots measured in this study, the Poisson's ratio was set to 0.33. This ratio was chosen after a survey of previous literature involving imaging of polymers and soft substrates using atomic force microscopy nanoindentation techniques, which established ~0.33 as the approximate range of appropriate Poisson's ratio values for the measurement of moduli in soft substrates and polymer gels[21–25]. Young's modulus ± standard deviation is reported for each group.

Evaluation of in vitro fibroblast migration within clots treated with PLPs + ultrasound

Neonatal human dermal fibroblasts (HDFn) (Gibco, Waltham, MA, USA) (P8-P13) were cultured into collagen/fibrinogen matrices composed of 3 mg/mL bovine collagen type I

(PureCol™ EZ gel solution, Sigma-Aldrich, St. Louis, MO, USA) and 1 mg/mL human fibrinogen (FIB 3, Enzyme Research Laboratories, South Bend, IN, USA) in a 12-well tissue culture plate (CELLTREAT Scientific Products, Pepperell, MA, USA) for 24 hours in a modification of an *in vitro* wound healing assay developed by Chen *et al*[26]. Following the 24-hour culture period, a 2 mm biopsy punch (VWR, Radnor, PA, USA) attached to a vacuum line was used to create a wound defect in the center of each well. 10 μL of clot solution (either control fibrin clots, ULC clots, or PLP clots) was added into each defect. The defect areas were imaged immediately using a light microscope (t = 0 hrs) and then allowed to polymerize for one hour. After 1 hour of polymerization, HDFn growth medium (DMEM, 10% fetal bovine serum, 1% penicillin-streptomycin, 1% L-glutamine) was added into each well and ultrasound was applied to +US clots for 30 minutes. The defect areas were imaged again 2 hours after initial clot formation, and cell infiltration back into the defect was quantified using the ImageJ cell counter. A total of 6 independent samples were run per condition. Average cell count in the defect area ± standard deviation is reported for each group.

Determination of PLP + US combinatorial therapy on wound healing in vivo

In vivo wound healing in the presence of ultrasound and PLP combinatorial treatment was evaluated through application of Dunn *et al.*'s full-thickness dermal injury model[27] to 8 week old C57BL6 mice (Charles River Laboratories, Wilmington, MA, USA). Mice were anesthetized using general anesthesia (5% isoflurane in oxygen) for the duration of surgery. 4 mm biopsy punches (Fisher Scientific, Hampton, NH, USA) were used to excise full-thickness dermal wounds that extended through the panniculus carnosus. Unlike human wound healing, murine wound healing occurs via skin contraction rather than re-epithelialization; to more accurately model human wound healing, wounds were splinted using silicone rings with a 10 mm outer diameter and 5 mm inner diameter, ensuring that wounds would heal via re-epithelialization. PLPs were delivered topically to wounds via 10 μL clot matrices. Standard fibrin clots, ULC clots, and 0.9% sterile filtered saline treatments were administered as control treatments. Wounds were imaged macroscopically using a digital camera, and then ultrasound was applied for 30 minutes; following ultrasound application, wounds were covered in waterproof, but water vapor permeable, Opsite bandages (Fisher Scientific, Hampton, NH, USA). Wounds were imaged and Opsite bandages were changed daily for the duration of the study. Carprofen (5 mg/kg) was administered subcutaneously for pain relief, once prior to removal of mice from anesthesia and then daily for five days post-surgery. Nine days post-surgery, mice were sacrificed, and wound tissue was harvested and fixed in 10% formalin. Wound tissues were then dehydrated through ascending serial ethanol dilutions, paraffin-embedded, and sectioned for histological and immunohistochemical analysis.

Wound size analysis was performed on wound images taken daily and then blinded by treatment group and randomized using a random number generator. Wound boundaries were determined manually via differences in tissue color and texture, and sizes were determined using ImageJ image analysis software to trace wound boundaries. Wound areas were normalized to the standardized area of the silicone ring openings in order to account for

variations in imaging position prior to determining closure rates for wounds in each treatment group.

Martius Scarlet Blue (MSB) staining was performed on wound tissue sections to identify fibrin and collagen within the wound area. Epidermal thickness was quantified from MSB slides in ImageJ by measuring the epidermal layer thickness at 5 regions spaced evenly across the wound. CD31 immunolabeling was also performed on tissue sections in order to assess angiogenesis occurring within the wound areas. Following deparaffinization and rehydration, tissue sections were blocked in 1% goat serum (Thermo Fisher Scientific, Waltham, MA, USA) in PBS. After blocking, sections were labeled 1:50 with a monoclonal antibody to CD31 (clone SP38, Thermo Fisher Scientific, Waltham, MA, USA) and incubated overnight at 4 °C. Sections were washed 3X in PBS and then incubated with an Alexa 594 secondary antibody (Thermo Fisher Scientific, Waltham, MA, USA) for one hour at room temperature. Sections were again washed 3X in PBS, then mounted with Vectashield Hardset mounting medium with DAPI (Fisher Scientific, Hampton, NH, USA). CD31+ tissue was quantified using the ImageJ Particle Analysis tool to measure total red areas greater than 1.0 μm^2 with an intensity threshold of 0–50. To assess macrophage polarization within wound sections, sections were blocked in 3% goat serum and co-labeled 1:500 using a polyclonal antibody to pan-macrophage marker CD68 (Thermo Fisher Scientific, Waltham, MA, USA) and either 1:200 with a monoclonal antibody to M1 marker CD86 (clone GL1, Thermo Fisher Scientific, Waltham, MA, USA) or 1:20 with a polyclonal antibody to M2 marker mMMR/CD206 (Fisher Scientific, Hampton, NH, USA)[28]. Sections were incubated overnight at 4 °C, washed 3X, and then incubated for one hour at room temperature with Alexa 488 and an Alexa 594 secondary antibodies to allow visualization of the pan-macrophage marker and either the M1 or M2 marker, respectively. Sections were washed 3X in PBS and mounted using Vectashield Hardset mounting medium with DAPI.

For each wound healing parameter, a minimum of four wounds were analyzed per treatment group (n = 4 for saline, ULC, fibrin + ultrasound, and ULC + ultrasound groups; n = 5 for fibrin and PLP groups; n = 6 for PLP + ultrasound group), with three sections analyzed per wound. Average ± standard deviation is reported for each parameter. All procedures were approved by the North Carolina State University IACUC.

Statistical analysis

Statistical analysis was performed using GraphPad Prism 8 (GraphPad, San Diego, CA, USA). Outlier tests were performed on all datasets prior to statistical analysis and graph creation using a ROUT outlier test with Q = 1%. Data for all experiments was analyzed through a one-way analysis of variance (ANOVA) with a Tukey's post hoc test using a 95% confidence interval.

Supplementary Material

Refer to Web version on PubMed Central for supplementary material.

Author Manuscript

Acknowledgements:

References

1. Modery-Pawlowski CL; Tian LL; Pan V; McCrae KR; Mitragotri S; Sen Gupta A, Approaches to synthetic platelet analogs. Biomaterials 2013, 34 (2), 526–541. [PubMed: 23092864]

2. Tutwiler V; Litvinov RI; Lozhkin AP; Peshkova AD; Lebedeva T; Ataullakhanov FI; Spiller KL; Cines DB; Weisel JW, Kinetics and mechanics of clot contraction are governed by the molecular and cellular composition of the blood. Blood 2016, 127 (1), 149–159. [PubMed: 26603837]

3. Cines DB; Lebedeva T; Nagaswami C; Hayes V; Massefski W; Litvinov RI; Rauova L; Lowery TJ; Weisel JW, Clot contraction: compression of erythrocytes into tightly packed polyhedra and redistribution of platelets and fibrin. Blood 2014, 123 (10), 1596–1603. [PubMed: 24335500]

4. Weisel JW; Litvinov RI, Mechanisms of fibrin polymerization and clinical implications. Blood 2013, 121 (10), 1712–1719. [PubMed: 23305734]

5. Nandi S; Sproul EP; Nellenbach K; Erb M; Gaffney L; Freytes DO; Brown AC, Platelet-like particles dynamically stiffen fibrin matrices and improve wound healing outcomes. Biomaterials Science 2019, 7 (2), 669–682. [PubMed: 30608063]

6. Stanworth SJ; Estcourt LJ; Powter G; Kahan BC; Dyer C; Choo L; Bakrania L; Llewelyn C; Littlewood T; Soutar R; Norfolk D; Copplestone A; Smith N; Kerr P; Jones G; Raj K; Westerman DA; Szer J; Jackson N; Bardy PG; Plews D; Lyons S; Bielby L; Wood EM; Murphy MF, A No-Prophylaxis Platelet-Transfusion Strategy for Hematologic Cancers. New England Journal of Medicine 2013, 368 (19), 1771–1780. [PubMed: 23656642]

7. Wandt H; Schaefer-Eckart K; Wendelin K; Pilz B; Wilhelm M; Thalheimer M; Mahlknecht U; Ho A; Schaich M; Kramer M; others, Therapeutic platelet transfusion versus routine prophylactic transfusion in patients with haematological malignancies: an open-label, multicentre, randomised study. The Lancet 2012, 380 (9850), 1309–1316.

8. Brown AC; Stabenfeldt SE; Ahn B; Hannan RT; Dhada KS; Herman ES; Stefanelli V; Guzzetta N; Alexeev A; Lam WA; Lyon LA; Barker TH, Ultrasoft microgels displaying emergent platelet-like behaviours. Nature Materials 2014, 13 (12), 1108–1114. [PubMed: 25194701]

9. Lin B; Yin T; Wu YI; Inoue T; Levchenko A, Interplay between chemotaxis and contact inhibition of locomotion determines exploratory cell migration. Nat Commun 2015, 6, 6619. [PubMed: 25851023]

10. Joshi A; Nandi S; Chester D; Brown AC; Muller M, Study of poly (N-isopropylacrilamide-co-acrylic acid) (pNIPAM) microgel particle induced deformations of tissue mimicking phantom by ultrasound stimulation. Langmuir 2017, 1457–1465.

11. Chernysh IN; Everbach CE; Purohit PK; Weisel JW, Molecular mechanisms of the effect of ultrasound on the fibrinolysis of clots. J Thromb Haemost 2015, 13 (4), 601–609. [PubMed: 25619618]

12. Suchkova V; Carstensen EL; Francis CW, Ultrasound enhancement of fibrinolysis at frequencies of 27 to 100 kHz. Ultrasound in Medicine and Biology 2002, 28 (3), 377–382. [PubMed: 11978418]

13. Suchkova V; Siddiqi Farhan N; Carstensen Edwin L; Dalecki D; Child S; Francis Charles W, Enhancement of Fibrinolysis With 40-kHz Ultrasound. Circulation 1998, 98 (10), 1030–1035. [PubMed: 9737524]

14. Engler AJ; Sen S; Sweeney HL; Discher DE, Matrix Elasticity Directs Stem Cell Lineage Specification. Cell 126 (4), 677–689. [PubMed: 16923388]

15. Tse JR; Engler AJ, Stiffness Gradients Mimicking In Vivo Tissue Variation Regulate Mesenchymal Stem Cell Fate. PLOS ONE 2011, 6 (1), e15978. [PubMed: 21246050]

16. Mi B; Liu G; Zhou W; Lv H; Zha K; Liu Y; Wu Q; Liu J, Bioinformatics analysis of fibroblasts exposed to TGF−β at the early proliferation phase of wound repair. Mol Med Rep 2017, 16 (6), 8146–8154. [PubMed: 28983581]

17. Lam WA; Chaudhuri O; Crow A; Webster KD; Li T-D; Kita A; Huang J; Fletcher DA, Mechanics and contraction dynamics of single platelets and implications for clot stiffening. Nature Materials 2011, 10 (1), 61–66. [PubMed: 21131961]

18. Chee E; Nandi S; Nellenbach K; Mihalko E; Snider DB; Morrill L; Bond A; Sproul E; Sollinger J; Cruse G; Hoffman M; Brown AC, Nanosilver composite pNIPAm microgels for the development of antimicrobial platelet-like particles. Journal of Biomedical Materials Research Part B: Applied Biomaterials 2020, n/a (n/a).

19. Sproul E; Hannan RT; Brown AC, Characterization of fibrin-based constructs for tissue engineering In Biomaterials for Tissue Engineering: Methods and Protocols, Methods in Molecular Biology, Chawla K, Ed. Springer: 2018; Vol. 1758, pp 85–99.

20. Nellenbach K; Guzzetta NA; Brown AC, Analysis of the structural and mechanical effects of procoagulant agents on neonatal fibrin networks following cardiopulmonary bypass. Journal of Thrombosis and Haemostasis 2018, 16 (11), 2159–2167. [PubMed: 30182421]

21. Wang G; Crawford K; Turbyfield C; Lam W; Alexeev A; Sulchek T, Microfluidic cellular enrichment and separation through differences in viscoelastic deformation. Lab on a Chip 2015, 15 (2), 532–540. [PubMed: 25411722]

22. Park S; Lee YJ, Nano-mechanical compliance of Müller cells investigated by atomic force microscopy. Int J Biol Sci 2013, 9 (7), 702–706. [PubMed: 23904794]

23. Geissler E; Hecht AM, The Poisson Ratio in Polymer Gels. Macromolecules 1980, 13 (5), 1276–1280.

24. Duong H; Wu B; Tawil B, Modulation of 3D fibrin matrix stiffness by intrinsic fibrinogen-thrombin compositions and by extrinsic cellular activity. Tissue Eng Part A 2009, 15 (7), 1865–1876. [PubMed: 19309239]

25. Lai VK; Lake SP; Frey CR; Tranquillo RT; Barocas VH, Mechanical behavior of collagen-fibrin co-gels reflects transition from series to parallel interactions with increasing collagen content. Journal of biomechanical engineering 2012, 134 (1), 011004–011004. [PubMed: 22482659]

26. Chen Z; Yang J; Wu B; Tawil B, A Novel Three-Dimensional Wound Healing Model. Journal of Developmental Biology 2014, 2 (4), 198–209.

27. Dunn L; Prosser HCG; Tan JTM; Vanags LZ; Ng MKC; Bursill CA, Murine Model of Wound Healing. J Vis Exp 2013, (75), 50265.

28. Pineda Molina C; Giglio R; Gandhi RM; Sicari BM; Londono R; Hussey GS; Bartolacci JG; Quijano Luque LM; Cramer MC; Dziki JL; Crapo PM; Badylak SF, Comparison of the host macrophage response to synthetic and biologic surgical meshes used for ventral hernia repair. Journal of Immunology and Regenerative Medicine 2019, 3, 13–25.
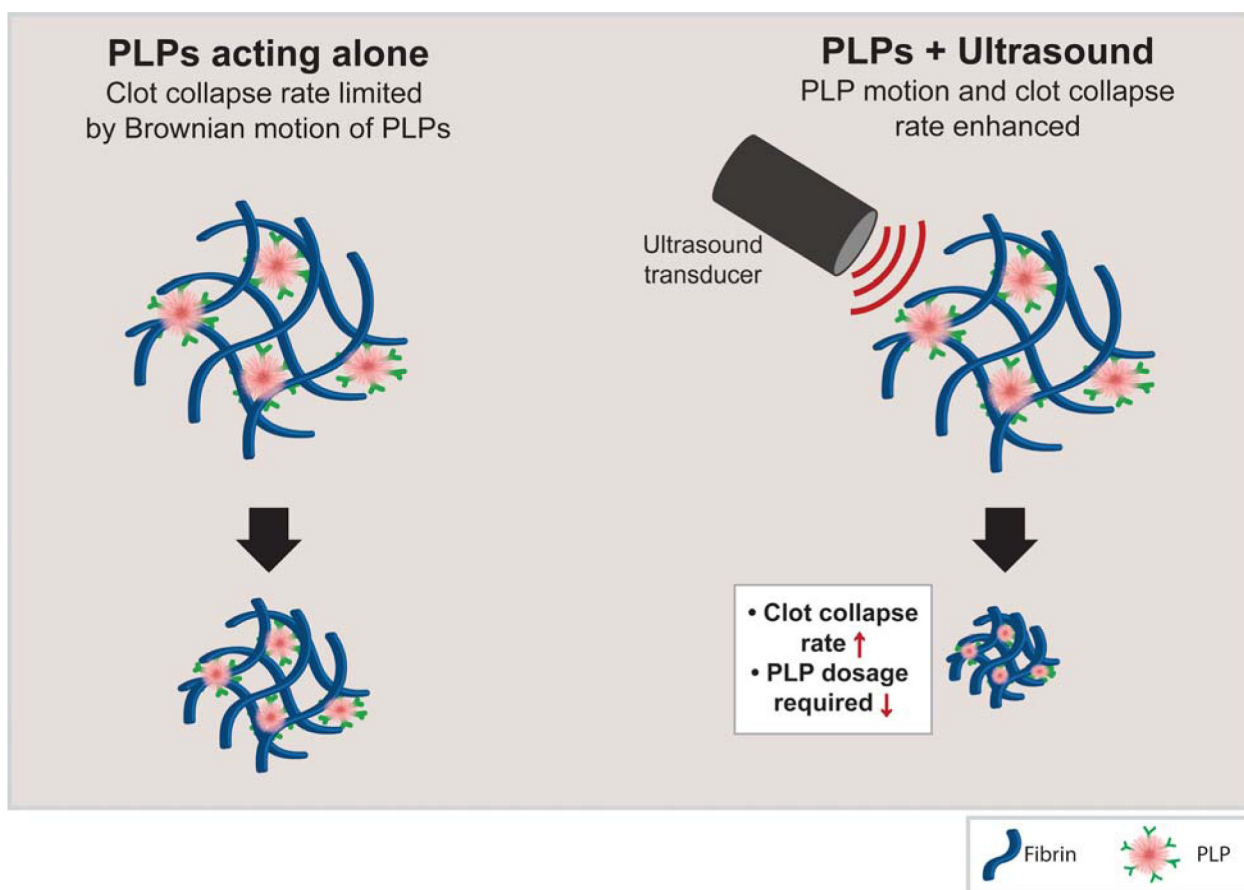
Figure 1: PLP motion is enhanced by the addition of ultrasound stimulation.
PLPs bind fibrin fibers via anti-fibrin antibodies and induce clot contraction through a Brownian wrench mechanism (left). When ultrasound stimulation is applied, we hypothesize that PLP deformation is increased within the fibrin network, increasing the rate of PLP-fibrin binding and thus increasing the rate at which clot contraction occurs.
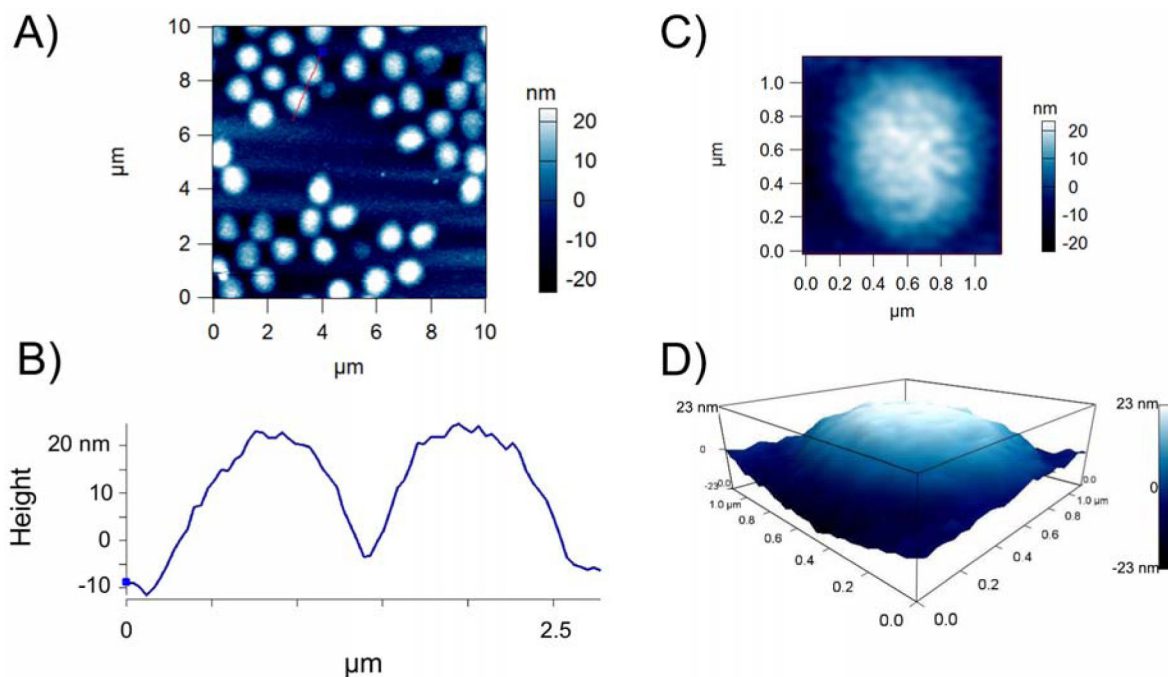
Figure 2: AFM characterization of ULC microgels deposited on a glass coverslip demonstrate ULC microgels are highly deformable.

A) ULC microgels synthesized using 90% NIPAm and 10% AAc were deposited on a glass coverslip and imaged via AFM dry imaging. On glass surfaces, microgels were found to deform to have diameters on the order of 1 micron and B) to flatten to low heights of 26.5 ± 21.7 nm. C) A representative single ULC microgel deposited on a glass coverslip. D) 3D map of the single ULC particle shown in part C. n = 30 particles analyzed.
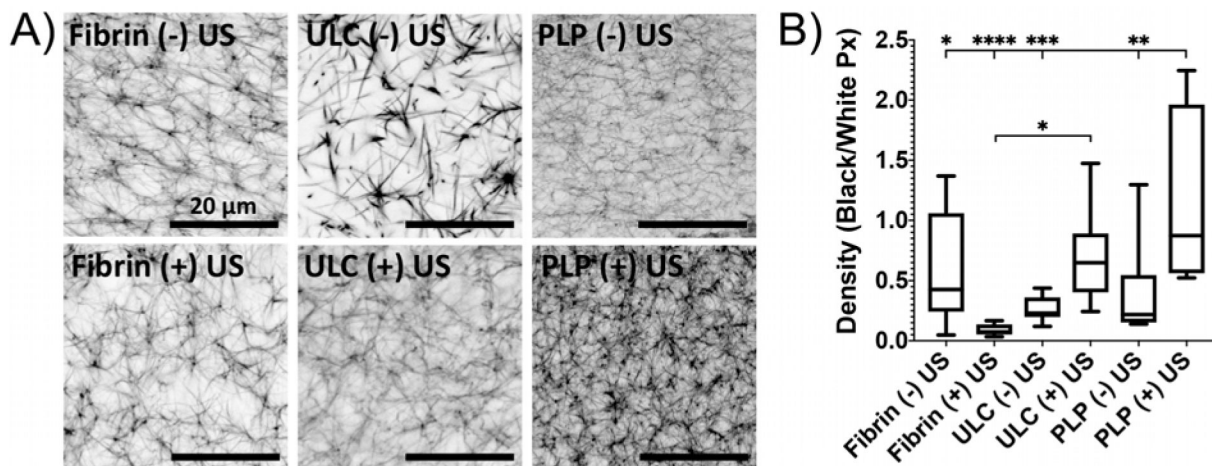
Figure 3: Clot density is increased in clots treated with both PLPs and ultrasound.
A) Confocal microscopy of fibrin clots taken at 63X magnification illustrates that the combination of a low dosage of PLPs in combination with ultrasound significantly enhances clot network density relative to fibrin-only clots +/− US and clots containing non-fibrin targeting ULC microgels +/− US. B) Clot network density was determined by dividing the total area of fibers (black pixels) over negative space (white pixels) within images binarized using a threshold of 150–255. n = 4 clots per group with 3 images analyzed per clot. Mean +/− standard deviation are presented. *p < 0.05; **p<0.01; ***p<0.001; ****p<0.0001.
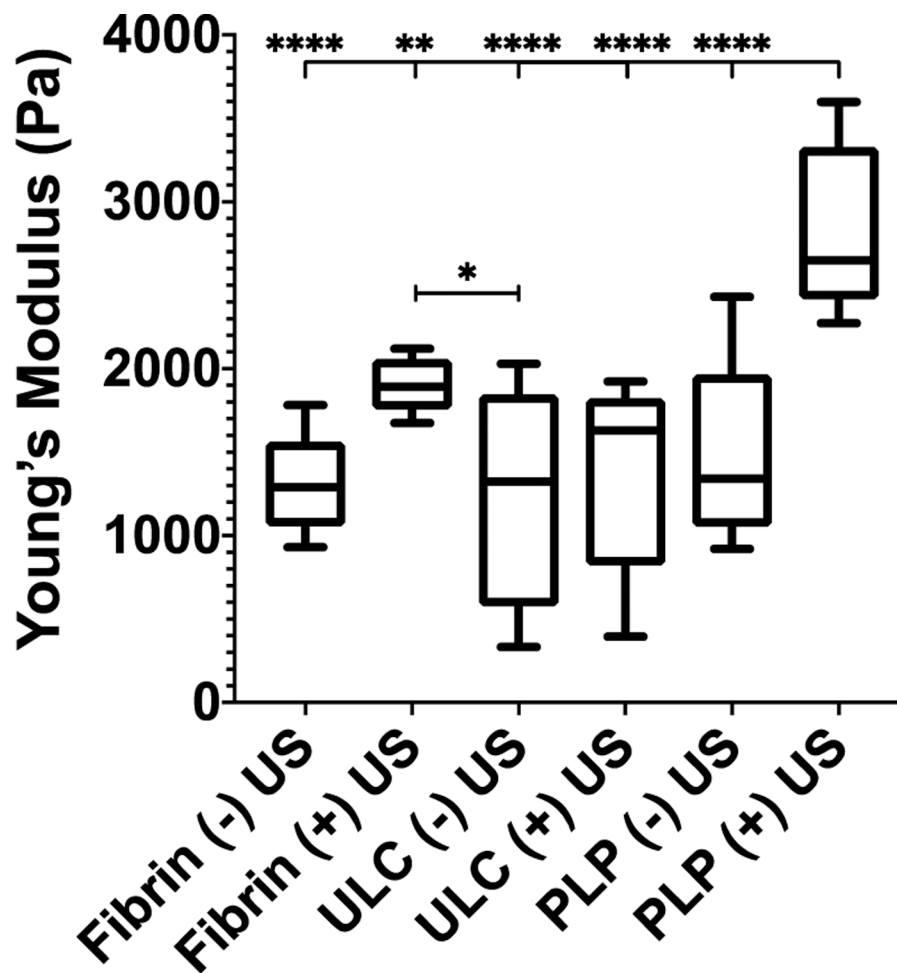
Figure 4: Clot stiffness increases in the presence of combined PLP and ultrasound treatment.
AFM force mapping of fibrin clots obtained 2 hours after initial polymerization reveals that
the Young's modulus of fibrin clots incorporated with PLPs and exposed to ultrasound is
significantly increased relative to control fibrin clots +/− US, non-fibrin targeting ULC
microgel-laden clots +/− US, and PLP-laden clots not exposed to US. n = 3 clots per group
with 3 random locations imaged per clot. Mean +/− standard deviation are presented. *p <
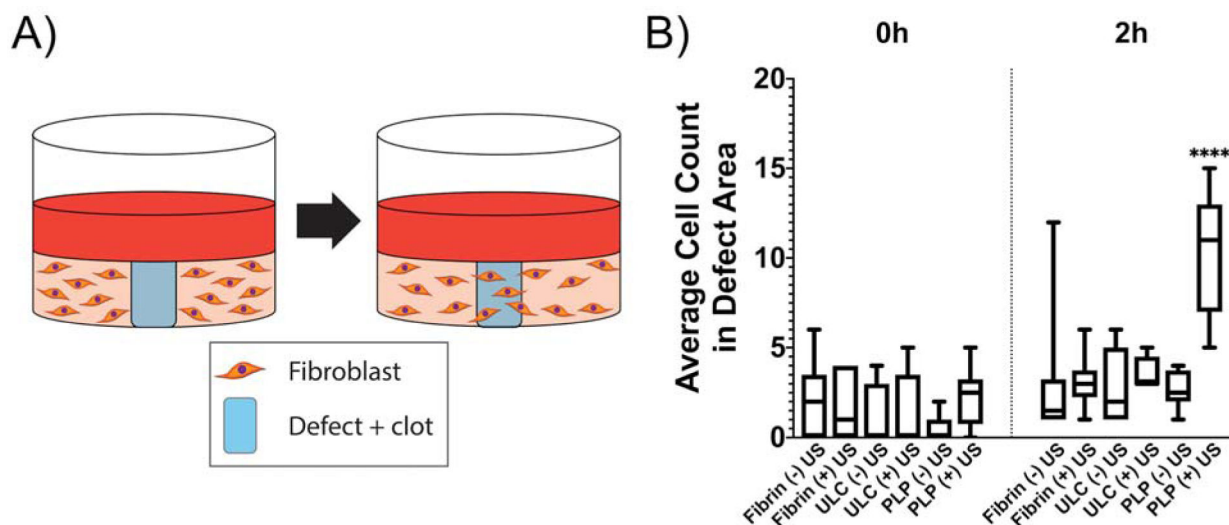0.05; **p < 0.01; ****p < 0.0001.

Figure 5: *In vitro* **fibroblast migration increases within clots treated with PLP + ultrasound treatment.**

A) Schematic of experimental design. Defects were induced in collagen/fibrinogen matrices seeded with neonatal human dermal fibroblasts (HDFns) and filled with fibrin clots. Two hours after induction of the defect, cell migration back into the defect area was determined via brightfield microscopy. B) Fibroblast migration into the defect area is significantly increased in defects filled with fibrin clots containing PLPs and exposed to ultrasound with respect to all other groups. Mean +/− standard deviation are represented. n = 6 per condition. ****p < 0.0001.
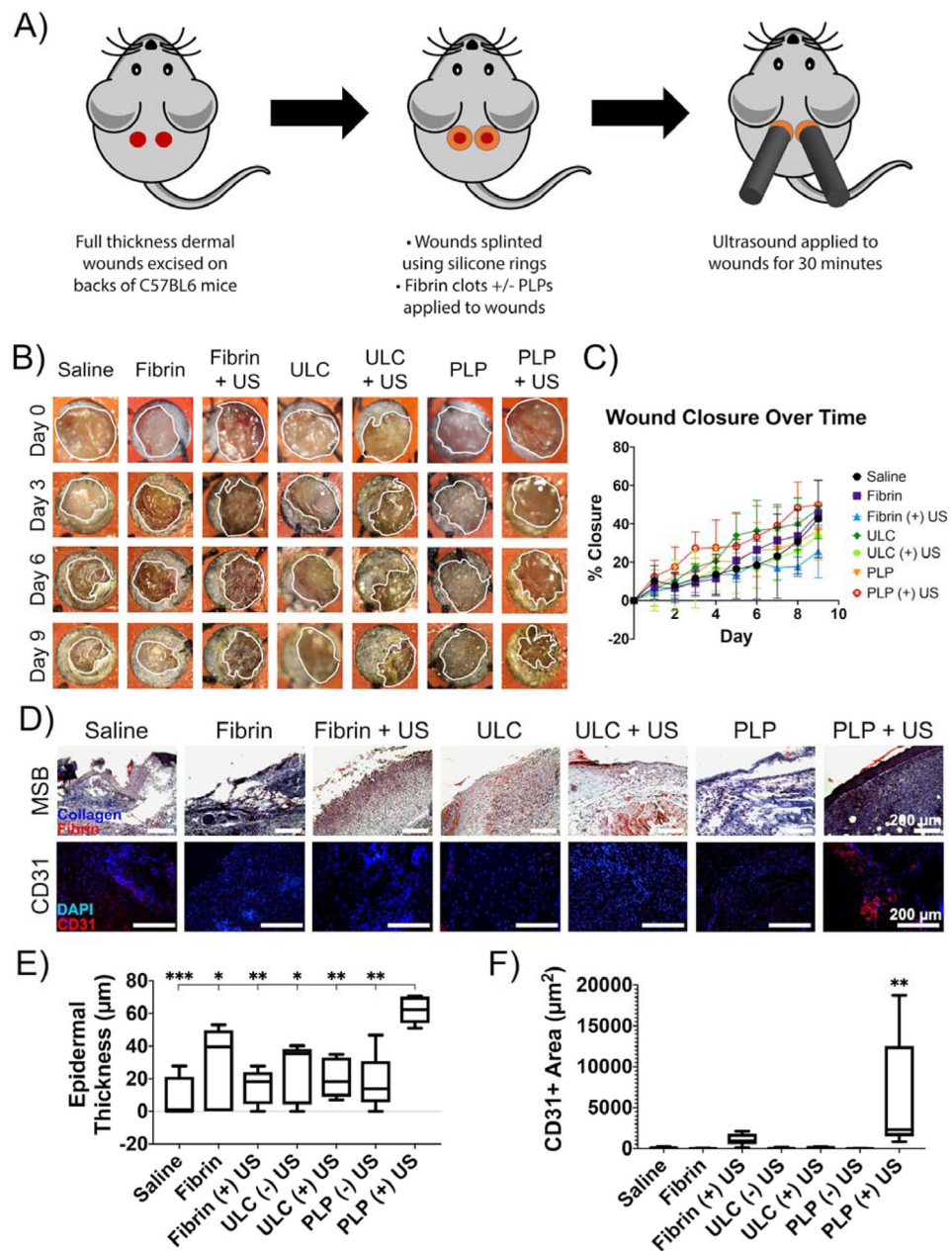
Figure 6: PLP + ultrasound treatment results in improved markers of wound healing *in vivo*.
A) Schematic of *in vivo* set-up. Ultrasound is applied to full thickness dermal wounds on the backs of 8 week old male C57BL6 mice for 30 minutes and then wound closure is monitored daily for 9 days post-injury. B) Representative macroscopic images of wounds taken at Days 0, 3, 6, and 9 following topical application of treatments +/− ultrasound. Wound borders are shown in white. C) Percent wound closure was calculated from wound tracings. D) Histological and immunohistochemical labeling of wound tissues reveals that epidermal thickness and angiogenesis are enhanced in tissues treated with both PLPs and ultrasound relative to tissues treated with fibrin-only clots +/− US, non-fibrin targeting ULC microgel-laden clots +/− US, and PLP-laden clots not exposed to US. E) Epidermal thickness is likewise enhanced in wound tissues treated with both PLPs and ultrasound

relative to controls. F) Total CD31 positively-labeled tissue is also increased in wound tissues treated with both PLPs and ultrasound relative to controls. Mean +/− standard deviation are represented for all graphs. n = 4–6 wounds per treatment group. *$p < 0.05$; **$p < 0.01$; ***$p < 0.001$; ****$p < 0.0001$.
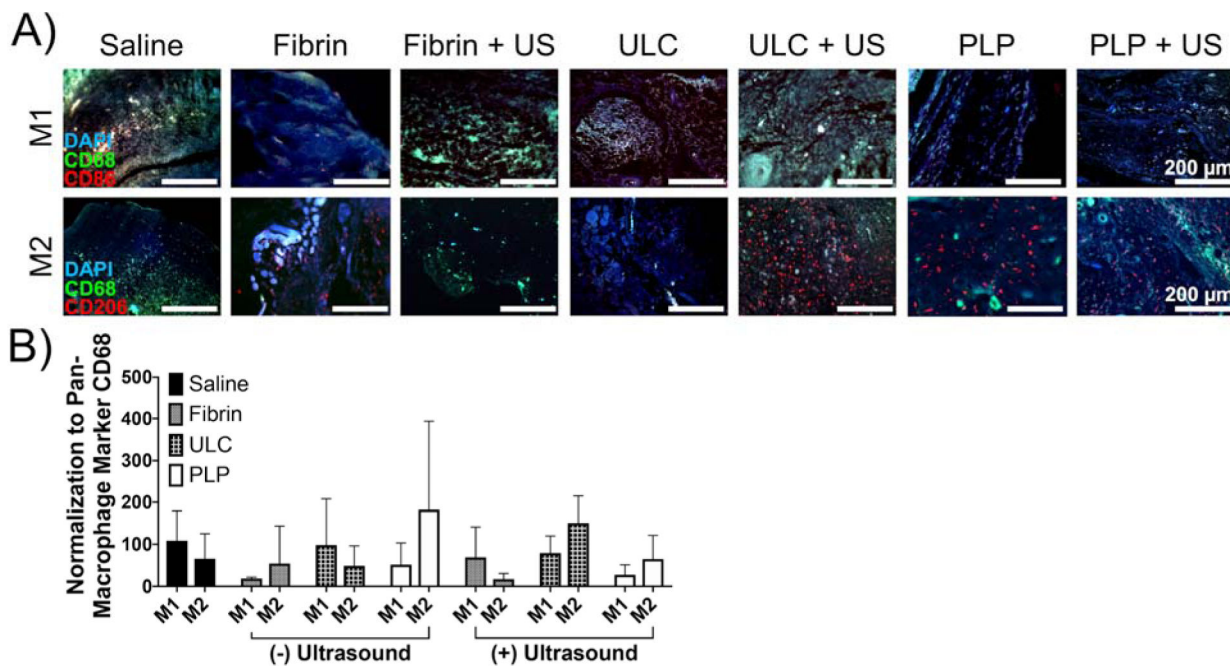
Figure 7: Immunohistochemical labeling of pan-macrophage marker CD68 and M1 or M2 marker CD86 or CD206 illustrate variations in macrophage polarization among treatment groups.

Macrophage polarization among treatment groups is varied, although no significant trends are visible as a result of wound treatment. Mean +/− standard deviation is represented. n = 4–6 wounds per treatment group.